SOFT X-RAY SASE AND SELF-SEEDING STUDIES FOR A NEXT-GENERATION LIGHT SOURCE

G. Penn*, P.J. Emma, D. Prosnitz, J. Qiang, M. Reinsch, LBNL, Berkeley, CA 94720, USA

Abstract

In the self-seeding scheme, the longitudinal coherence and spectral density of an unseeded FEL can be improved by placing a monochromator at a location before the radiation reaches saturation levels, followed by a second stage of amplification. The final output pulse properties are determined by a complex combination of the monochromator properties, undulator settings, variations in the electron beam, and wakefields. We perform simulations for the output of SASE and self-seeded configurations for a soft x-ray FEL using both idealized beams and realistic beams from start-to-end simulations.

INTRODUCTION

The longitudinal coherence and spectral density of a SASE FEL can be improved without using an external seed by introducing a monochromator in the middle of the undulator beamline [1]. The narrow bandwidth selected by the monochromator will act as a seed in the following undulators, leading to a final bandwidth that can be much narrower than the original SASE bandwidth. A hard X-ray version of such a device [2] has been implemented and tested at LCLS [3]. A soft X-ray self-seeding beamline is currently under development for implementation at LCLS as well [4]. Here, simulations of a soft x-ray self-seeded beamline are presented using a beam tracked from an RF injector through a superconducting (SC) linac.

SELF-SEEDING SCHEME

The self-seeding scheme, shown in Fig. 1, breaks the SASE configuration into two parts, with a monochromator and chicane in between. The noisy SASE bunching is eliminated by the chicane, and the monochromator selects a narrow bandwidth to seed the second stage. The monochromator should be roughly in the middle of the undulator length, constrained to be far enough downstream so that enough power gets through the monochromator to overcome shot noise, but not too far that the increased energy spread of the beam entering the second stage seriously degrades the FEL performance. To reach saturation, the total undulator length must be increased from that of a SASE beamline by enough to compensate for the following effects: the reduction in radiation power due to both the narrower bandwidth; losses or mismatch in the radiation transport; an effective loss in power by a factor of roughly 9 as some of the radiation field couples to FEL modes which do not get amplified; and the increased gain length in the second stage due to the increase in energy spread. For a monochromator with a

_____
* gepenn@lbl.gov

bandwidth selection of around 20 meV, for a relative bandwidth of a few times 10^{-5}, and a 10% transport efficiency in this bandwidth, an extra 5 undulator sections (16 m of undulator) are required. Overall, there is a factor of almost 10^4 in power amplification, which corresponds to around 9 gain lengths, that must be added to the FEL beamline.

Only planar undulators are considered; polarization control can be obtained through the use of cross-planar undulators at the very end of the beamline [5]. The current design places two such undulator sections at the end of the beamline for maximum flexibility. The possibility of additional undulators are added to the beginning and end of the beamline to account for expected imperfections, such as undulator field errors and steering errors which are allowed a budget of a 10% increase in gain length, and unknown effects which may degrade the electron beam quality or the efficiency of the monochromator.

BEAMLINE PARAMETERS

The nominal parameters and those obtain in full start-to-end (S2E) simulations starting from the injector [6] and passing through a SC linac [7] are shown in Table 1. However, the beamlines are designed to be able to handle a worse beam emittance, of up to 0.9 μm, as well as an energy spread of 150 keV. The energy spread is adjustable by the use of a laser heater [8], to damp out microbunching instabilities.

Table 1: Electron beam parameters, both original nominal parameters and results from S2E simulations. Except for bunch charge, parameters correspond to typical values in the core region of the bunch.

	Nominal	S2E core
Bunch charge	300 pC	300 pC
Electron energy	2.4 GeV	2.4 GeV
Slice energy spread	100 keV	90 keV
Slice transverse emittance	0.60 μm	0.75 μm
Peak current	600 A	450 A

The beamline is designed to cover the range in photon energies from 270 eV (just below the Carbon K-edge) up to 1.24 keV. We focus on undulators using superconducting (SC) technology with relatively short undulator period, to provide the full tuning range with reasonably large (not much smaller than unity) dimensionless undulator parameter at the highest photon energy. SC undulators have the advantage of being able to produce higher magnetic fields for a larger gap, especially for undulator periods shorter
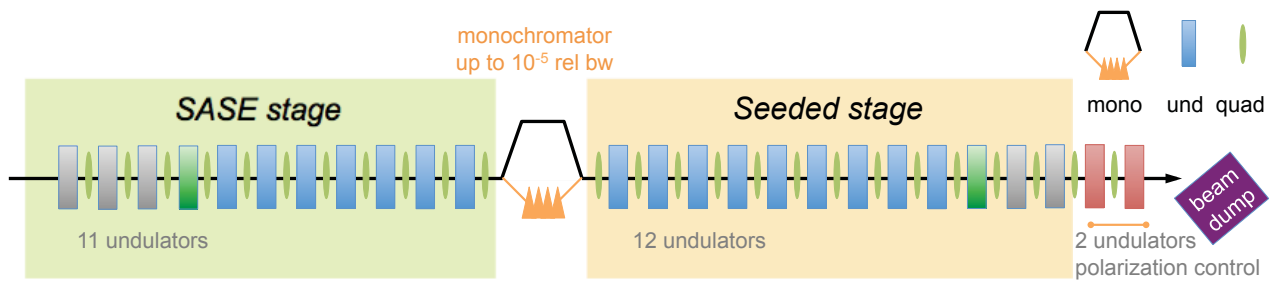
Figure 1: A schematic of the self-seeding configuration. The last two undulator sections are for polarization control. The two before that are contingency in case the beam quality is worse than expected, as are the first three undulator sections. An additional undulator before and after the monochromator are to make up for steering and undulator errors, which have not been included in the simulation.

than 30 mm. This allows for more compact beamlines, and lower energy beams, and larger undulator parameters. There is also the possibility that SC undulators will be more robust to the environment resulting from a high average beam power that could approach 1 MW. The undulator period is taken to be 19.4 mm, and the magnetic gap between undulators is 7.5 mm, which allows the inner diameter of the beampipe to be 6 mm. Each undulator section has a length of 3.3 m, with breaks of 1.1 m containing a quadrupole, phase shifter, diagnostics, and orbit correctors.

At a resonant photon energy of 1.24 keV, the gain length is 2.0 m, and the effective FEL parameter is 4×10^{-4}. The effective shot noise power is 35 W. To ensure that shot noise is strongly suppressed in the second stage, we intend to keep the seeding power delivered by the monochromator above 100 times this value, or 3.5 kW.

START-TO-END SIMULATIONS

Simulations for a 300 pC electron bunch have been performed from the injector through the first set of cryomodules for acceleration using the ASTRA code. These particles have then been tracked through the linac and spreader using Elegant. The longitudinal beam distribution at the entrance of the undulators is shown in Fig. 2. Although a model for the laser heater has been included in these studies, the full range of self-forces which lead to longitudinal instabilities have not been included, so the microbunching instability is not accurately modelled. Nevertheless, the FEL performance should not be significantly affected if a modest additional increase in initial energy spread is required.

The FEL itself is modeled using the GENESIS simulation code [9], plus a simplified model for the monochromator which assumes a narrow enough selected bandwidth that the resulting radiation pulse is nearly coherent both longitudinally and transversely. At the entrance to the monochromator, the radiation at 1.24 keV has of order 100 SASE spikes, with peak powers at the level of 10 MW. The total pulse energy is 1.8 μJ. If continued to saturation, the total pulse energy would grow to 140 μJ. The assumed

monochromator performance reduces the bandwidth to the point where the seed pulse going in to the next undulator is close to the transform limit, the pulse energy is reduced to 1.8 nJ, and the peak power is roughly 4 kW. In contrast to SASE radiation, the temporal profile is smooth as well.
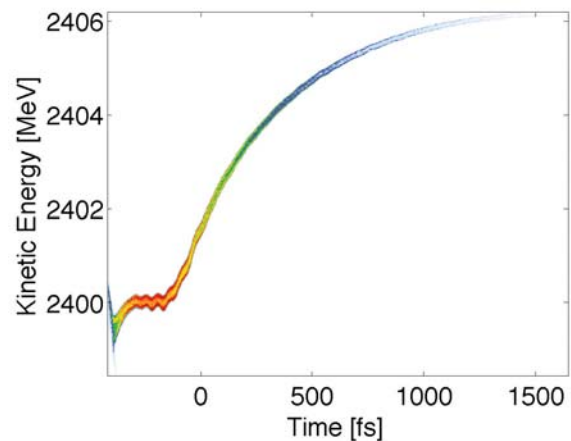

Figure 2: Longitudinal phase space of the beam entering the FEL. Insignificant power is generated for $t > 0$, and this region is not included in simulations.

In the second stage, the radiation remains mostly coherent and grows to 210 μJ. The resulting spectrum is shown in Fig. 3, with a FWHM bandwidth of 25 meV; most of the power lies within a range of 70 meV. By contrast, the spectrum for an equivalent SASE simulation is shown in Fig. 4. Without the monochromator, the bandwidth is of the order of 1 eV, and the individual spikes will vary shot to shot. Even the strongest spikes in the spectrum are over an order of magnitude below the self-seeded spectrum in terms of spectral density.

To understand the reason for the presence of radiation outside of the monochromator bandwidth, it is necessary to look at the variation of the slice average energy with longitudinal position. In addition to the initial longitudinal distribution at the first undulator, resistive wall wake-
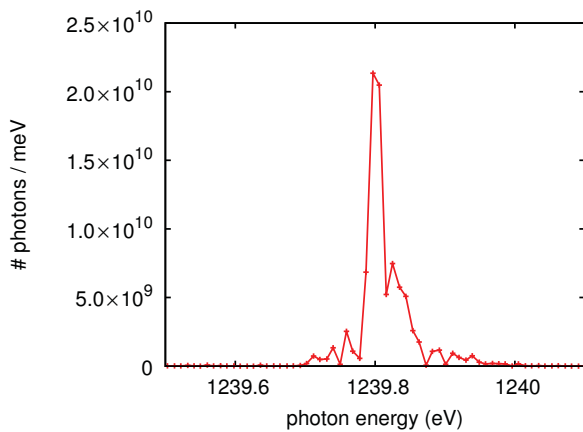
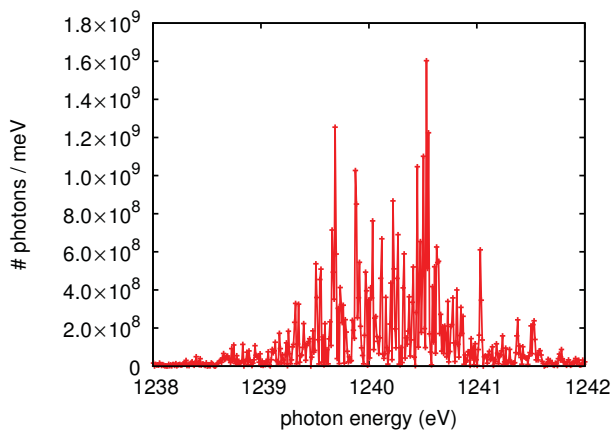Figure 3: Spectrum from a full S2E run for the self-seeded beamline.

Figure 4: Spectrum from a full S2E run for a basic SASE beamline. The total length of undulator used is 36 m. Note the difference in horizontal scale.

fields induce additional energy chirps in the electron beam as it propagates through the undulators. The small beam pipe diameter of 6 mm causes these wakes to be significant. In these simulations, the wakes were calculated using a model for cold copper ($\sim$ 4K) which takes into account the anomalous skin depth effect.

These energy variations lead to position-dependent shifts in radiation phase, as seen in Fig. 5. The regions where the radiation phase is flat correspond to the flat regions in the original energy profile and in the resistive wall wake fields. The beam used here had less bunch compression applied to it than in the nominal configuration. One benefit of lengthening the bunch is to lengthen the flat regions in the bunch. Additionally, the peak wake field near the head of the pulse due to the "impulse" of the onset of the bunch mostly misses the target region of the beam where the current is high. These two benefits together allow for a long section of the output pulse with a fairly flat phase. Finally, reducing the peak current reduces the magnitude of both the wakes and energy offsets. The amplitude of the en-

ergy variations maps directly to the amplitude of the phase modulations, which in this case are mostly held to a range of ± 1 radian, except for the region around -100 fs where there is a "knee" in the longitudinal distribution. This region near the tail of the high-current core of the beam is the largest contributor to the distortion of the laser seed coming out of the monochromator.

A good approximation for the shift in phase due to energy deviations in the electron bunch is given by:

$$\Delta\theta \simeq 0.6 \times 4\pi \, \frac{L_u - 1.5L_g}{\lambda_u} \, \eta \,, \qquad (1)$$

where η is the relative energy offset from the optimal value. This expression holds in the exponential regime where the growing mode dominates over the other modes, but before saturation. At saturation, and even near saturation, not only does the rate of phase slippage decrease but the energy offsets themselves begin to damp out due to nonlinear effects. Linear 1D theory yields a factor of 2/3 rather than 0.6. The phase shift of an electron relative to a nominal plane wave is given by the same expression without the factor of 0.6. Thus, the actual phase drift can be viewed as the electrons and radiation field adopting a compromise phase between their natural values. Because wake fields lead to a linear change in energy with propagation distance, they will introduce a quadratic dependence of phase on undulator length, but the process is the same.

CONCLUSIONS

A start-to-end example of a soft x-ray self-seeded FEL has been studied based on an electron beam simulated from the injector to the final beam energy. This example has been shown to yield only a small increase of the bandwidth beyond that selected by the monochromator. The good coherence of the x-ray pulse was achieved by reducing the bunch compression in the linac from the nominal value, in order to make the slice energy more uniform through the high-current portion of the pulse. Other techniques for improving the coherence of the output pulse should be evaluated, in order to allow for higher peak current in the core of the electron bunch if so desired.
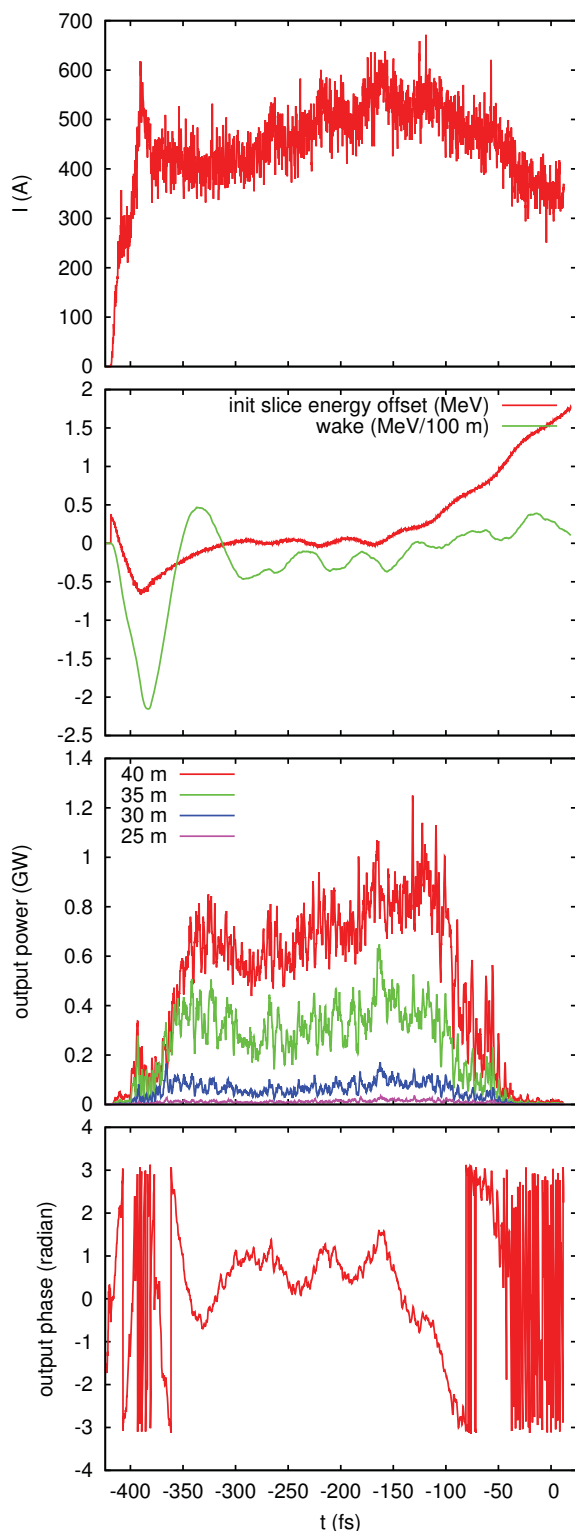
Figure 5: Temporal profile of electron beam current and slice energy deviation, resistive wall wakefield forces, and laser pulse power and phase.

REFERENCES

[1] J. Feldhaus, E.L. Saldin, J.R. Schneider, E.A. Schneidmiller, and M.V. Yurkov, Optics Commun.140 (1997) 341–352.

[2] G. Geloni, V. Kocharyan, and E. Saldin, J. Modern Optics 58 (2011) 1391–1403.

[3] J. Amann, W. Berg, V. Blank, F.-J. Decker, et al., Nature Photonics (2012) 180, doi:10.1038/nphoton.2012.180.

[4] J. Wu, P. Emma, Y. Feng, J. Hastings, and C. Pellegrini, "Staged self-seeding scheme for narrow bandwidth, ultra-short x-ray harmonic generation free electron laser at Linac Coherent Light Source," in *Proceedings of FEL2010, Malmö, Sweden*, Sweden, 2010, paper TUPB08, pp. 266–269.

[5] K.-J. Kim, Nucl. Instrum. Methods A 445 (2000) 329–332.

[6] C.F. Papadopoulos, J. Corlett, P. Emma, D. Filippetto, et al., "Injector beam dynamics for a high-repetition rate 4th-generation light source," in *Proceedings of IPAC2012, New Orleans, LA, USA*, New Orleans, 2010, paper WEPPR031, pp. 3000–3002.

[7] M. Venturini, J. Corlett, P. Emma, C. Papadopoulos, et al., "Beam dynamics studies of a high-repetition rate linac-driver for a 4th generation light source," in *Proceedings of IPAC2012, New Orleans, LA, USA*, New Orleans, 2010, paper TUPPP074, pp. 1771–1773.

[8] Z. Huang, A. Brachmann, F.-J. Decker, Y. Ding, et al., Phys. Rev. ST Accel. Beams 13 (2010) 020703.

[9] S. Reiche, Nucl. Instrum. Methods A 429 (1999) 243–248.